



Modular Conjugation of a Potent Anti-HER2 Immunotoxin Using Coassociating Peptides

Audrey Stoessel, Nadja Groysbeck, Lucile Guyot, Lina Barret, Yves Nominé,
Leonel Nguekeu Zebaze, Ambre Bender, Laetitia Voilquin, Thomas Lutz,
Nikita Pallaoro, et al.

► To cite this version:

Audrey Stoessel, Nadja Groysbeck, Lucile Guyot, Lina Barret, Yves Nominé, et al.. Modular Conjugation of a Potent Anti-HER2 Immunotoxin Using Coassociating Peptides. *Bioconjugate Chemistry*, 2020, 31 (10), pp.2421-2430. 10.1021/acs.bioconjchem.0c00482 . hal-03005245

HAL Id: hal-03005245

<https://hal.science/hal-03005245>

Submitted on 13 Nov 2020

HAL is a multi-disciplinary open access archive for the deposit and dissemination of scientific research documents, whether they are published or not. The documents may come from teaching and research institutions in France or abroad, or from public or private research centers.

L'archive ouverte pluridisciplinaire **HAL**, est destinée au dépôt et à la diffusion de documents scientifiques de niveau recherche, publiés ou non, émanant des établissements d'enseignement et de recherche français ou étrangers, des laboratoires publics ou privés.

Modular conjugation of a potent Anti-HER2 immunotoxin using co-associating peptides

Audrey Stoessel¹, Nadja Groysbeck¹, Lucile Guyot^{2,3}, Lina Barret², Yves Nominé⁴, Leonel Nguekeu-Zebaze¹, Ambre Bender¹, Laetitia Voilquin⁴, Thomas Lutz¹, Nikita Pallaoro¹, Marie Blocat¹, Celia Deville⁴, Murielle Masson¹, Guy Zuber¹, Bruno Chatton¹, and Mariel Donzeau^{1*}.

1 Université de Strasbourg, UMR7242 Biotechnologie et Signalisation Cellulaire, Ecole Supérieure de Biotechnologie Strasbourg, F-67412 Illkirch, France.

2 IMPReSs Facility, Biotechnology and Cell Signaling, CNRS – University of Strasbourg, Illkirch, F-67412 Illkirch, France.

3 NovAliX, Bioparc, F-67405 Illkirch, France

4 Institut de Génétique et de Biologie Moléculaire et Cellulaire, Illkirch, F-67400 Illkirch, France.

*mariel.donzeau@unistra.fr

Abstract:

Immunotoxins are emerging candidates for cancer therapeutics. These biomolecules consist of a cell targeting protein combined to a polypeptide toxin. Associations of both entities can be achieved either chemically by covalent bonds or genetically creating fusion proteins. However, chemical agents can affect activity and/or stability of the conjugate proteins and additional purification steps are often required to isolate the final conjugate from unwanted by-products. As for fusion proteins, they often suffer from low solubility and yield.

In this report, we describe a straightforward conjugation process to generate an immunotoxin using co-associating peptides (named K3 and E3), originating from the tetramerization domain of p53. To that end, a nanobody targeting the human epidermal growth factor receptor 2 (nano-HER2) and a protein toxin fragment from *Pseudomonas aeruginosa* Exotoxin A (TOX) were genetically fused to the E3 and K3

peptides. Entities were produced separately in *E. coli* in soluble forms and at high yields. The nano-HER2 fused to the E3 or K3 helices (nano-HER2-E3 and nano-HER2-K3) and the co-assembled immunotoxins (nano-HER2-K3E3-TOX and nano-HER2-E3K3-TOX) presented binding specificity on HER2 overexpressing cells with relative binding constants in the low nanomolar to picomolar range. Both toxin modules (E3-TOX and K3-TOX) and the combined immunotoxins exhibited similar cytotoxicity levels compared to the toxin alone (TOX). Finally, nano-HER2-K3E3-TOX and nano-HER2-E3K3-TOX evaluated on various breast cancer cells were highly potent and specific to kill HER2-overexpressing breast cancer cells with IC₅₀ values in the picomolar range. Altogether, we demonstrate that this non-covalent conjugation method using two co-assembling peptides can be easily implemented for modular engineering of immunotoxins targeting different types of cancers.

Keywords: immunotoxin, co-assembly, peptide, HER2, cytotoxicity.

INTRODUCTION

The human epidermal growth factor receptor 2 (HER2) is a cell surface receptor overexpressed in about 15-20% of breast cancers. Amplification of HER2 is associated with tumor invasion and metastasis. Introduction of an anti-HER2 therapy using the humanized monoclonal antibody trastuzumab targeting specifically the extracellular domain of HER2 has largely improved patient care.¹ However, intrinsically or acquired resistance has restricted the success of the trastuzumab.^{2,3} Since two decades, new anti-HER2 therapies have been under investigation. One emerging therapeutic is immunotoxins, which combine the specific targeting of antibodies with the high cytotoxic properties of bacterial or plant protein toxins.⁴⁻⁶ Upon specific binding to extracellular receptors and receptor-mediated endocytosis, immunotoxins get internalization into target cells, where the toxin domain unfolds its effect. These therapeutic biomolecules have demonstrated excellent anti-cancer properties at very low concentrations due to the enzymatic activity of the toxin fragment, which lowers the amount of molecules needed to kill cancer cells.^{7,8} One of the most widely used toxin fragments originates from *Pseudomonas aeruginosa* exotoxin A. It contains separate activities: a domain II for intracellular trafficking and a

catalytic domain (domain III) inactivating the eukaryotic translation elongation factor 2 (eEF-2) by ADP-ribosylation.⁹

Immunotoxins can be produced as chimeric proteins. For instance, an affibody, an antibody mimetic molecule, directed against HER2 genetically fused to a modified exotoxin A fragment PE38 showed elevated cytotoxicity towards HER2 overexpressing cells.^{10,11} However, the weakness of such an approach is the expression level and the solubility issue of the recombinant immunotoxins. To overcome these problems, both the targeting and toxin moieties can be produced separately and are then chemically conjugated.^{12,13} For example, the scFv (single chain variable fragment) of trastuzumab and a minimal exotoxin A fragment (PE24) that were expressed independently and conjugated via a disulfide bond-containing linker, had strong cytotoxic effects on HER2 breast cancer cells.¹³ But the drawback of such an approach is the use of reducing agents, leading to improper protein folding, and therefore lowering solubility and/or activities of the conjugate proteins. Moreover, additional purification steps are required to isolate the desired conjugate from by-products present in the conjugation mixture. These additional purification steps often result in low yields and make the chemical conjugation a time-consuming and cost ineffective process.

In this study, we report a novel straightforward conjugation procedure based on co-assembly of a single chain antibody (nanobody or VHH) targeting HER2 receptor and a truncated variant of the exotoxin A from *Pseudomonas aeruginosa* via two peptides (named E3 and K3), originating from the tetramerization domain of p53 (residues 325-355).¹⁴ These peptidic domains consist of a β -strand followed by a α -helix. The α -helical charged interface involving lysine and acid glutamic residues (E343, E346 and K351) modulates tetramer stability through salt bridges. Thus charge-reversal mutations at positions 343, 346 and 351 was previously shown to favor heterotetramerization.¹⁵ While E3 (variant E343, E346 and E351) associates solely into dimers through β -strand interactions, K3 (variant K343, K346 and K351) forms tetramers with low stability. However, when mixed together in equimolar amounts, these peptides associate exclusively into dimer of primary dimers. This non-covalent interaction between E3 and K3 peptides was demonstrated to be strong and specific enough to allow heterotetramerization of macromolecules inside living cells for the engineering of bifunctional bio-molecules.¹⁶ Using this technology to co-assemble a nanobody anti-HER2 with a truncated optimized fragment of the exotoxin

A from *Pseudomonas aeruginosa*, we generate extremely stable heterotetrameric immunotoxins having a specific cytotoxic activity on HER2 positive breast cancer cells.

RESULTS

Design of the immunotoxin

We designed novel immunotoxins able to co-assemble via E3 and K3 peptides (Figure 1A and B).¹⁶ We choose a nanobody targeting the extracellular domain of HER2 (henceforth referred to as nano-HER2).^{17,18} The nano-HER2 sequence was genetically fused to the N-terminal part of K3 sequence (Figure 1A).¹⁶ The selected toxin module derives the *Pseudomonas* exotoxin A variant PE24,^{19,20} where the intracellular trafficking domain has been replaced by a furin cleavage site (FCS) described elsewhere²¹, and the B-cell epitopes and the protease-sensitive regions have been removed.²⁰ This toxin part (hereinafter referred to as TOX) was then genetically fused to the C-terminal part of the E3 peptide (Figure 1A). The design of the immunotoxin was also carried out to obtain the opposite configuration, namely nano-HER2-E3 combined with K3-TOX, given rise to nano-HER2-E3K3-TOX (Figure 1B).

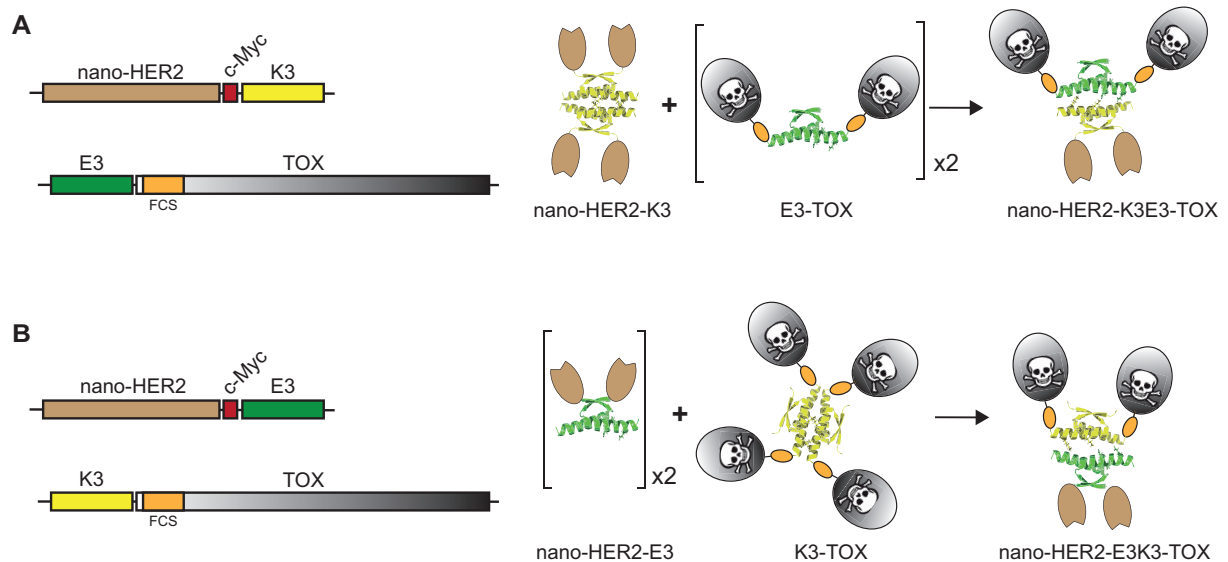


Figure 1: Representations of heterotetrameric immunotoxins. Schematic representation of either nano-HER2-K3E3-TOX (A) or nano-HER2-E3K3-TOX (B) co-assembled immunotoxins with coding sequences of each module, as indicated. Theoretical oligomerization states of the corresponding proteins, and the resulting co-assembled immunotoxins are depicted.

Production, yield and oligomeric states of the recombinant proteins

Recombinant VHH and TOX moieties were produced at high levels in *E. coli* (Figure S1A and S2A), and purified by immobilized metal affinity chromatography (IMAC) followed by a preparative size exclusion chromatography (SEC) (Figures S1B and C, and Figure S2B and C). Typical elution profiles revealed that the unfused nano-HER2 displayed a single peak with an apparent molecular weight of 21 kDa corresponding to a theoretical molecular weight of a monomer, while nano-HER2-E3 and nano-HER2-K3 behaved like a 63 kDa dimer and a 105 kDa tetramer, respectively (Figure 2A and Table S1). TOX constructs gave the same results in terms of oligomeric states, namely a homodimer of 68 kDa for E3-TOX and a homotetramer of 152 kDa for K3-TOX, respectively (Figure 2A). In all cases, single peaks were observed indicating an oligomerization state of nearly 100%. The final yields of the recombinant proteins after the two purification steps (Figures S1C and S2C) were around 100 mg/L for the nano-HER2-E3 and nano-HER2-K3, and in the range of 7 to 10 mg/L for the E3-TOX and K3-TOX (Table S2).

The secondary structure content of the recombinant proteins was next explored using far-UV circular dichroism (CD) spectroscopy, and the content of secondary structure elements was estimated using CDPPro suite software.²² The far-UV CD spectra of the tagged E3 and K3 constructs are highly similar (Figure 2B). The nano-HER2-E3 and the nano-HER2-K3 folded in $18\% \pm 1$ and $16\% \pm 1$ of α -helix, compared to $5\% \pm 2\%$ for the parental nano-HER2, indicating a rough increase of 27 to 32 amino acids in α -helix conformation per monomer (Figure 2B, and Table 1). These predictions are in agreement with previous results where adding E3 or K3 peptide to a con1 construct leads to an increased of almost 30 amino acid residues in α -helix.¹⁶ Regarding the TOX proteins, the α -helix portions increased in the similar way than for the nanobody constructs when compared to the parental TOX (Figure 2B and Table 1). Thus, secondary structures following addition of the E3 or K3 peptides stayed almost constant regardless of the constructs.

Finally, the thermal stability evaluation of the nano-HER2 recombinant proteins was performed using a fluorescence-based thermal shift assay (Figure S3). The melting profiles of the recombinant proteins were highly similar, indicating that fusion of the tagged constructs did not compromise the intrinsic stability of the VHH domain.

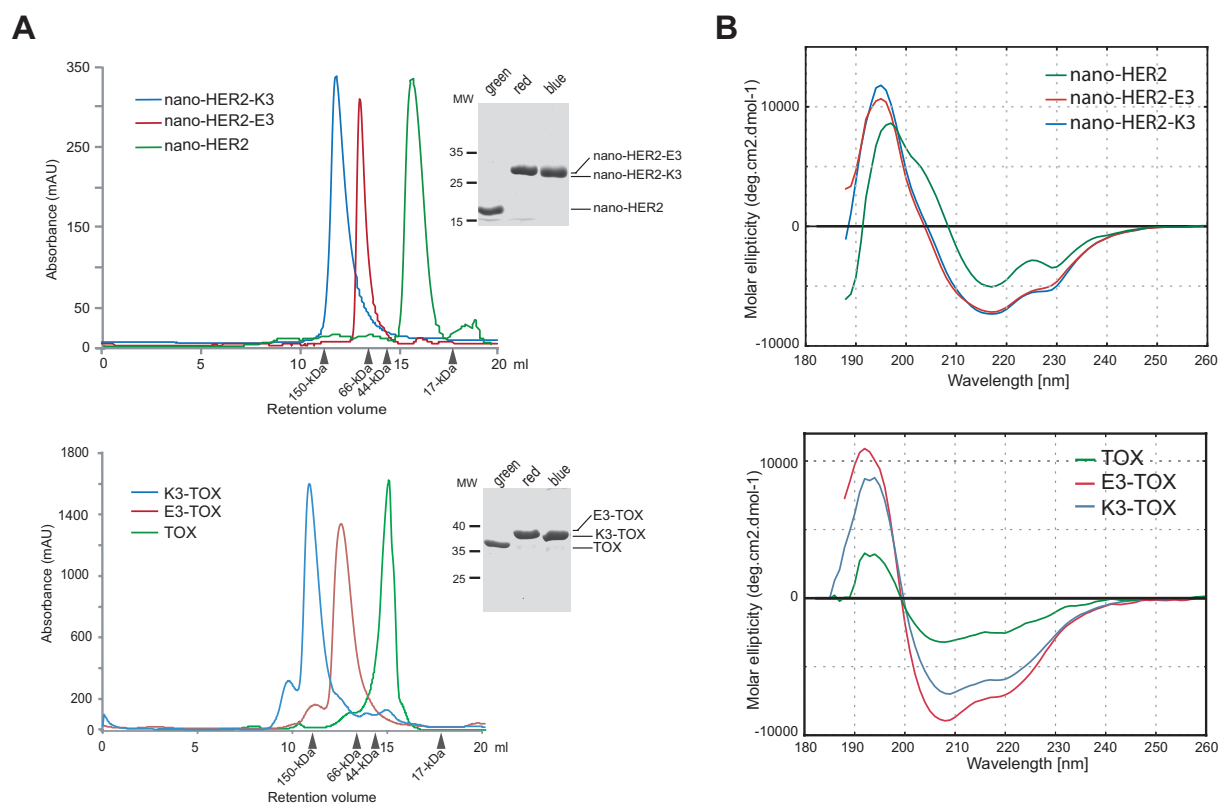


Figure 2. Physicochemical analysis of the K3 and E3 constructs. (A) Preparative gel filtration of purified nano-HER2 derivatives (above) and TOX constructs (below). The column was pre-calibrated with standard proteins as indicated (IgG, BSA, ovalbumin, and cytochrome C). A sample of each peak was analyzed by SDS-PAGE and by Coomassie blue staining. (B) Far-UV circular dichroism spectra of the indicated assemblies were recorded for samples at a monomeric concentration of 69 μ M in phosphate saline buffer and are presented as an average of ten successive scans. CD signal is expressed in mean residue ellipticity ($\text{deg}\cdot\text{cm}^2\cdot\text{dmol}^{-1}$). Data were collected in the 185–270 nm range at 20 °C.

Table 1: Secondary structure contents of the constructs: aa refers to the numbers of amino acids determined considering the percentage of each secondary structure content and assuming a single element.

	ALPHA		BETA		OTHERS	
	%	aa	%	aa	%	aa
Nano-HER2	5 \pm 2	7	41 \pm 8	61	54 \pm 9	79
Nano-HER2-E3	19 \pm 1	39	30 \pm 3	64	52 \pm 2	110
Nano-HER2-K3	16 \pm 1	34	33 \pm 3	70	51 \pm 3	109
TOX	7 \pm 2	20	39 \pm 3	114	54 \pm 4	156
E3-TOX	20 \pm 2	61	28 \pm 2	88	53 \pm 3	166
K3-TOX	17 \pm 1	53	31 \pm 2	98	52 \pm 2	164

In vitro formation of the heterotetramer complexes

Following the two purification steps, we studied the efficiencies of co-association between the nanobody and toxin modules in various conditions. Evaluation of modularity and efficiency of heteromerization were first analyzed in phosphate saline buffer at pH 7.4 using size exclusion chromatography (SEC). When equimolar amounts of either nano-HER2-E3 and K3-TOX, or nano-HER2-K3 and E3-TOX proteins were mixed together and analyzed by SEC, an apparent 125 kDa complex was produced, which was compatible with the theoretical molecular weight of the heterotetramer (Figure 3A and B, and Table S1). Thus, both elution profiles confirmed that the homotetramer dissociates to the benefit of a more stable heterotetrameric complex. As the extracellular micro-environment of a solid tumor is acidic,²³ the stability of the co-assembled immunotoxin nano-HER2-K3E3-TOX was assessed at low pH. Equimolar amount of nano-HER2-K3 and E3-TOX were mixed together and run on size exclusion chromatography in PBS pH 6. As shown in figure 3C, the nano-HER2-K3E3-TOX complex runs exactly at the same apparent molecular weight than the complex form at pH 7.4. Thus the nano-HER2-K3E3-TOX is stable at pH 6.

The quality of the protein assemblies in regard to colloidal stability was monitored by Dynamic Light Scattering analysis (DLS)(Figure S4). All complexes, including the heterotetramers display apparent hydrodynamic diameters of size below 14 nm with a low polydispersity index (PDI) in a range of 0.20, with the complete absence of unwanted protein-aggregates.

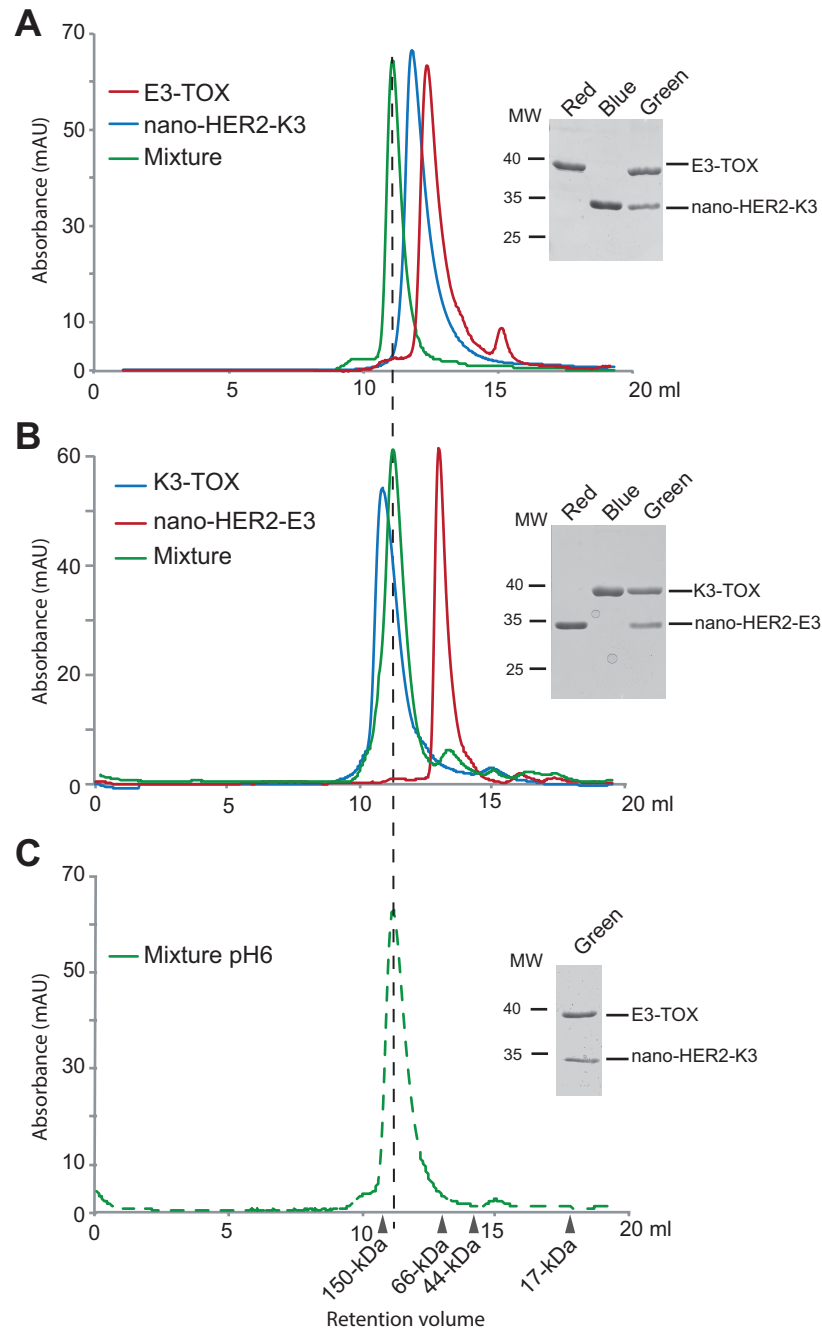


Figure 3. Co-association of the immunotoxins. Gel filtration of (A) purified nano-HER2-K3 (blue), E3-TOX (red), and a mixture of equimolar amounts of nano-HER2-K3 and E3-TOX (green), (B) purified nano-HER2-E3 (red), K3-TOX (blue), and a mixture of equimolar amounts of nano-HER2-E3 and K3-TOX (green), and analysis by SDS-PAGE and Coomassie blue staining of the peak fractions. (C) Gel filtration of co-assembled nano-HER2-K3/E3-TOX immunotoxin run at pH 6 (dotted green line) and SDS-PAGE and Coomassie staining analysis of the peak fraction.

The nanobodies and the co-associated immunotoxins retain cell-binding properties.

To assess whether the formation of heterodimers via E3 and K3 helices does not affect the binding of the nano-HER2, binding efficiencies of nanobodies and co-assembled immunotoxins were then measured on HER2-positive HCC1954 cells to determine relative binding constants. Thus, the recombinant proteins were randomly conjugated to NHS-Alexa488 dye via lysine residues and compared to the labeled parental nano-HER2 (Figure 4A and S5A). Following incubation with HCC1954 cells, fluorescence signals were measured using fluorescence-activated cell sorting (FACS). As shown in Figure 4B, monovalent nano-HER2 displayed an apparent binding constant (EC_{50}) of 21.8 nM (± 4.8), somewhat lower than the value previously described elsewhere on HER2-positive SKBR3 cells.¹⁷ The same experiment performed with the homodimer nano-HER2-E3 and the homotetramer nano-HER2-K3 exhibited relative binding efficiency values 1.0 nM (± 0.1) and 0.2 nM (± 0.1) indicating an increased binding efficiency of around 20- and 100-fold, respectively. These results pointed to an avidity effect of the dimer and tetramer nanobodies for improved binding to HER2 receptor. However, labeling either E3- or K3-TOX module prior assembly with the respective nanobody counterpart resulted in a significant drop in binding constants (Figure S5B). This result was likely due to a steric hindrance of the fluorophore preventing association between the toxin and the VHH modules as shown by analytical gel filtration (Figure S5C). Thus, labeling purified immunotoxin complexes resolved this issue (Figure S5). Indeed, Alexa488-labeled immunotoxin complexes displayed only a slight lower binding efficiency than their respective nanobody counterparts (Figure 4A and 4B). Nano-HER2-K3E3-TOX immunotoxin exhibited an EC_{50} of 2.5 nM \pm 0.3 and the nano-HER2-E3K3-TOX immunotoxin an EC_{50} of 3.7 nM \pm 0.4. No detectable binding was observed on HER2 low-expressing cells MDA-DB-231 or on HER2-silenced HCC1954 cells using small-interfering oligonucleotides (Figure S6A and S6B).

Overall, these results demonstrate the binding efficiency and specificity of the co-associated immunotoxins on HER2 cell surface receptor.

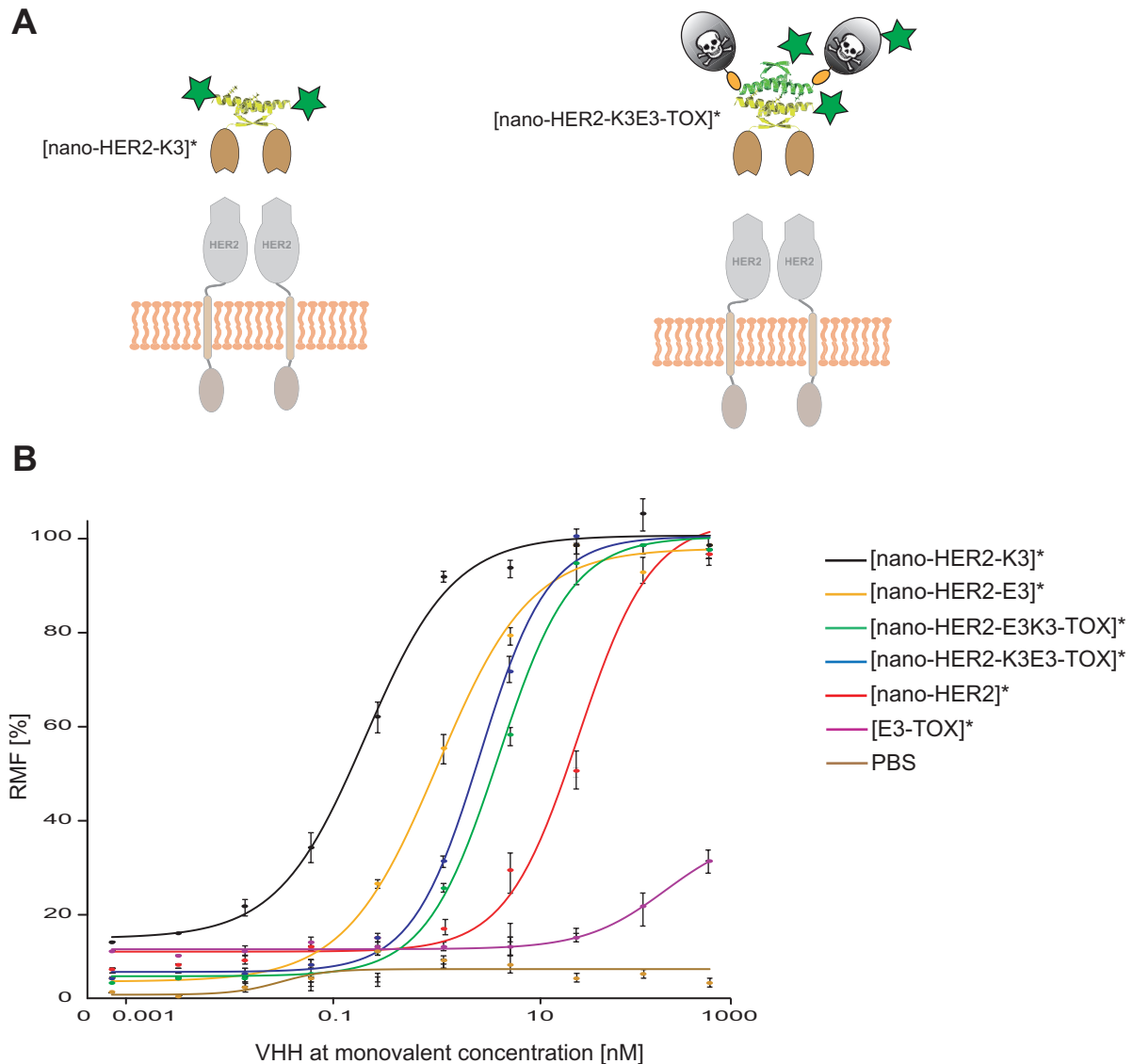


Figure 4. Apparent binding constants of the constructs on antigen-overexpressing cells. (A) Cartoon representing the binding of the labeled constructs [*] on HER2 cell surface receptor. (B) HCC1954 cells were titrated by increasing amounts of Alexa488-labeled recombinant proteins, as indicated [*]. Following incubation, the fluorescence was measured by fluorescence-activated cell sorting (FACS). The relative mean of fluorescence (RFM) was plotted against nanobody concentration (at monovalent concentration), and K_d values were determined using sigmoidal fitting with R software. ($n \geq 6$) and SD.

Co-assembly of the toxin with the nanobody via E3 or K3 peptides does not impair its cytotoxicity

Because oligomerization may harm the structural and functional integrity of the toxin, we evaluated the enzymatic activities of the toxins and the immunotoxins using an *in vitro* coupled transcription/translation assay using rabbit reticulocyte lysate and a luciferase reporter gene (Figure 5A). Increasing concentrations of either TOX, E3-

TOX, K3-TOX, or the co-assembled immunotoxins were added to the lysate in the presence of NAD⁺, the essential cofactor for the ADP-ribosylation of the eEF-2 elongation factor.²⁴ Translation efficiencies were monitored by measuring luciferase activities (Figure 5A). Determination of the inhibition dose-response curve yielded a half-inhibition (IC₅₀) at 235 pM (± 45) for the TOX comparable to the E3-TOX at 164 pM (± 30), and both co-assembled immunotoxins, HER2-E3K3-TOX and HER2-K3E3-TOX with IC₅₀ of 160 pM (± 15) and 260 pM (± 20), respectively. The homotetramer K3-TOX showed a slightly reduce inhibition activity with an IC₅₀ of 610 pM (± 50). Thus, addition of the helix and co-assembly of the nanobody with the toxin via E3 or K3 peptides did not compromise the enzymatic activity of the toxin.

The cytotoxic activity of all constructs were then also assessed by electro-transferring the recombinant proteins and complexes into various cell lines.²⁵ Both TOX and E3-TOX moieties yielded more than 90% of cell death after 72 h (Figure 5B). As a control, the transduced nano-HER2-E3 did not have any cytotoxic effects.

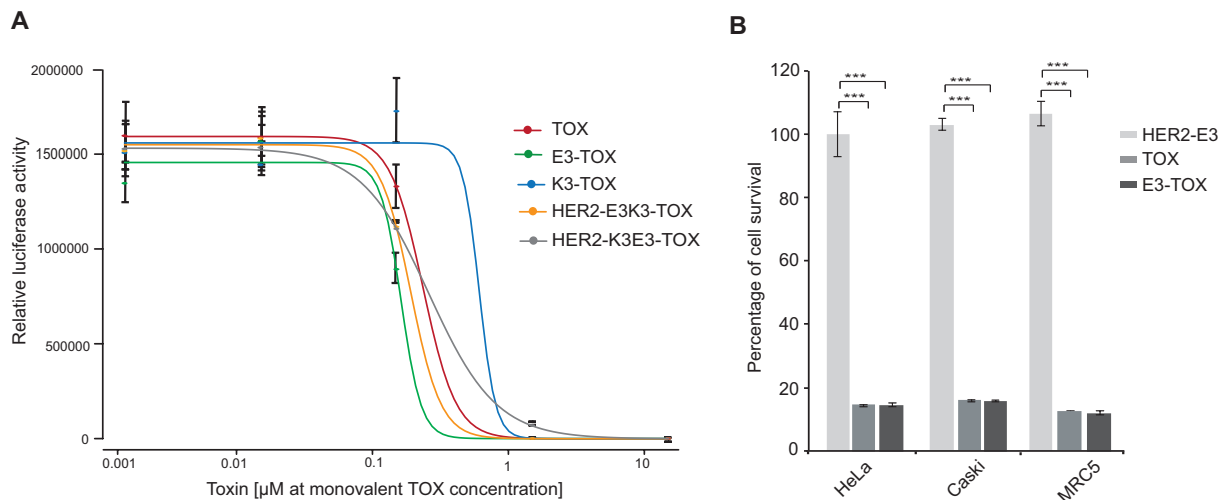


Figure 5: Cytotoxicity of the TOX modules. (A) Toxins and Immunotoxins inhibit protein translation. Recombinant proteins were tested in an *in vitro* transcription/translation assay using rabbit reticulocyte lysate and the luciferase activity as reporter. This assay was performed in triplicate. Sigmoidal curve fitting was performed using R software. (B) TOX and E3-TOX purified proteins were electro-transferred into various cell lines. After 72 h, cell viability was estimated as a percentage relative to cells transduced with PBS buffer. Analysis corresponds to at least an average of three independent experiments. Error bars represent standard deviations. Student's t-test was performed: *P<0.05, **P<0.01, ***P<0.001.

Specific cytotoxicity of the immunotoxins on HER2-positive breast cancer cells

Given the high binding affinity of the nano-HER2 for HER2 positive cancer cells and the high cytotoxicity of the TOX modules, we sought to determine the cytotoxicity of the co-assembled immunotoxins.

Thus, the cytotoxic effect and the specificity of the co-assembled immunotoxin, nano-HER2-K3E3-TOX, were evaluated on different breast cancer cell lines being either HER2-positive or HER2-negative. Three HER2-positive (HCC1954, BT474 and SKBR3), two HER2-negative (MCF7 and MDA-MB-231), and a non-human myoblastic cell line (H9C2(2-1) rat) were tested.²⁶ The cells were incubated for 72 h with increasing concentrations of either the immunotoxin nano-HER2-K3E3-TOX or the nano-HER2-K3 or the E3-TOX complexes (Figure 6A and 6B). The nano-HER2-K3E3-TOX revealed high cytotoxicity at picomolar levels on the HER2 overexpressing cell lines, compared to the toxin and to the VHH alone. The IC₅₀ values for BT474, HCC1954 and SKBR3 cells were 30 pM (\pm 4), 39 pM (\pm 15), and 160 pM (\pm 25), respectively ($n \geq 10$) (Figures 6A, and Table 2). The toxin alone, E3-TOX, had lower cytotoxic effects, in the range of 5 to 10 nM for HER2-positive cells and for MCF7 cells (Table 2). Thus the nano-HER2-K3E3-TOX immunotoxin was 185, 595 and 65 fold more potent on HCC1954, BT474 and SKBR3 cells, respectively, compared to the free toxin (E3-TOX) (Figure 6A and Table 2). No significant differences between the free toxin and the immunotoxin were noted in HER2-negative cells, supporting the notion that HER2 overexpression increases the uptake of the immunotoxin (Figure 6B and Table 2). In fact, MCF7, HER2-negative cell line, were affected to the same extent by the free toxin and by the immunotoxin with an IC₅₀ from 8.02 to 6.20 nM (\pm 0.15). Of note, the viability of MDA-MB-231 as well as H9C2(2-1) cell lines, was not affected by the immunotoxin (IC₅₀ \geq 300 nM) (Figure 6B, and Table 2). Similarly, the opposite configuration, namely the nano-HER2-E3K3-TOX displayed the same cytotoxicity as the nano-HER2-K3E3-TOX on HER2-positive cell lines and no effects on MDA-MB-231 (Figure S7 and data not shown).

The proteolytic stability of the constructs was also assessed by incubating both immunotoxins in 80% of serum (FBS) at 37 °C during 1, 5, 12 and 24 h. Immunotoxin cytotoxicity was then tested on HER2-positive HCC1954 cells. Nano-HER2-K3E3-TOX retained its full cytotoxic activity even after 24 h incubation in

serum at 37 °C with an IC₅₀ of 27.0 pM (\pm 6.3)(Figure 6C).

Altogether, these results indicate that the cytotoxicity of both immunotoxins is dependent on the specific association between the nano-HER2 and the toxin via the E3 and K3 helixes, and correlates with the presence of the HER2 receptor on the cell's surface. In addition, they show that the immunotoxin complexes are very stable at pH 6.00 as well as in serum.

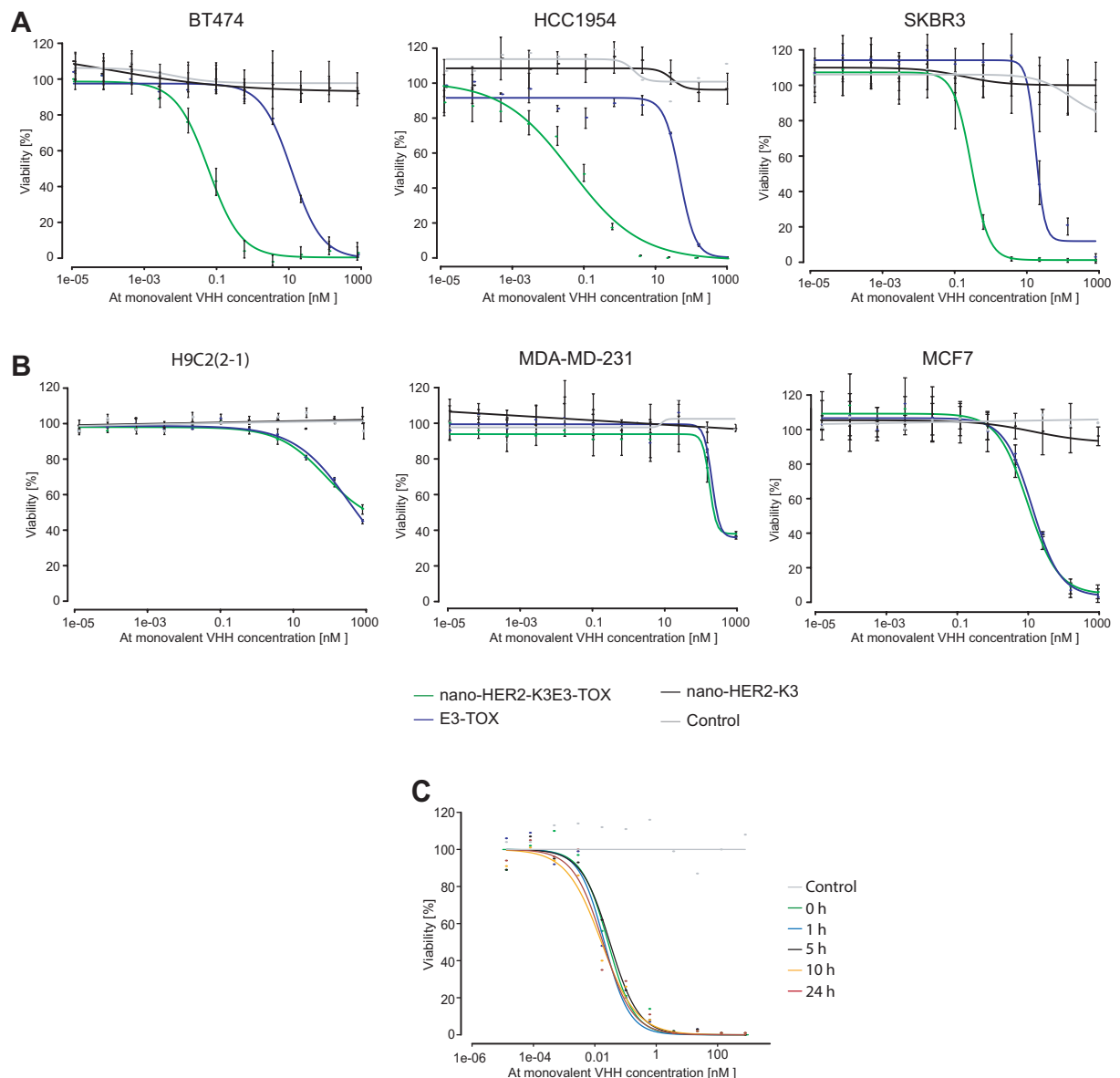


Figure 6. The immunotoxin nano-HER2-K3E3-TOX shows high cytotoxicity and specificity for HER2 overexpressing cells. (A) HER2-positive and (B) HER2-negative cells were treated for 72 h with the nano-HER2-K3E3-TOX, nano-HER2-K3, and E3-TOX alone ($n \geq 10$). (C) HER2-positive HCC1954 cells were treated for 72 h with the nano-HER2-K3E3-TOX previously incubated in 80 % serum at 37°C for

various times, as indicated. HER2 The relative cell viability to untreated cells was plotted against antibody concentrations, and IC₅₀ values were determined using sigmoidal fitting with R software.

Table 2. Cytotoxicity of the immunotoxin on target and control cells.

Bio-molecule	BT474	HCC1954	SKBR3	MDA-MB-231	MCF7
	IC ₅₀ (pM)	IC ₅₀ (pM)	IC ₅₀ (pM)	IC ₅₀ (pM)	IC ₅₀ (pM)
Nano-HER2-K3E3-TOX	30.0 ± 4.0	39.0 ± 15	160 ± 25	>300000	6250 ± 150
E3-TOX	5550 ± 80	16710 ± 150	10380 ± 230	>300000	8020 ± 150
Nano-HER2-K3	NA	NA	NA	NA	NA
Ratio ER	185	595	65	n.d.	n.d.

DISCUSSION

In this study, we developed a straightforward co-assembly technique to produce an immunotoxin combining a nanobody directed against HER2 and a toxin via two peptides E3 and K3.¹⁶ The non-covalent and highly specific pairing of the E3 and K3 peptides yielded to the generation of heterotetrameric immunotoxins, composed of two VHH and two toxin molecules. We clearly demonstrate that the engineered immunotoxins retain their specific binding and toxic properties, hence being specifically toxic for HER2-overexpressing breast cancer cells.

Because production of immunotoxins is impeded in eukaryotic cells due to their high toxicity, most engineering applications for their production relies on the design of chimeras produced in *E. coli*.^{10,11,20} However, fusion proteins often suffer from low solubility and low yield.^{10,27} For example, an affibody anti-HER2 fused to a PE38 fragment from the exotoxin A of *Pseudomonas aeruginosa* was not soluble and was purified from the inclusion bodies¹⁰ while a chimeric recombinant immunotoxin composed of a VHH directed against the vascular endothelial growth factor receptor 2 and the PE38 fragment was produced at a final yield of 9.2 mg / L.²⁷ Another strategy is to generate both moieties independently, which in addition to improved yield and solubility, makes it possible to produce the antibody domain in eukaryotic cells. Different protein conjugation strategies have been explored. For instance, a HER2-scFv fragment has been chemically conjugated to PE24 via N-succinimidyl-3-(2-pyridyldithio)propionate (SPDP).¹³ The HER2-(scFv)-PE24 end product was then

purified by size exclusion chromatography. However, the highest yield of the obtained conjugation was only 58% and required additional purification steps. An elegant protein *trans-splicing* (TPS) technology was also reported for the conjugation of either the Trastuzumab-targeted HER2 or two VHHs targeting different epitopes of HER1 (EGFR) to the PE24 fragment of the Exotoxin A from *Pseudomonas*.¹² Coupling efficiencies in the range of 50-70% were achieved and it was not possible to distinguish molecules with a toxin/antibody ratio of 2 from those with partial coupling. Finally, an additional step was also required to remove the unconjugated mAb.

The use of co-assembling peptides offers several significant advantages. Both moieties can be produced separately, overcoming solubility and yield issues reported for chimeric immunotoxins. Indeed, the VHH was produced at a yield of 100 mg/L and the toxin module showed a high solubility yield. In addition, neither reduction nor chemical conjugation is required, thereby avoiding subsequent purification steps, making it a very simple and convenient technology. Following assembly of the nano-HER2 and the toxin via E3 and K3, the heterotetramer immunotoxin complexes were able to efficiently and specifically kill HER2-expressing breast cancer cells. In addition, the bivalence format of the nanobody can probably trigger an efficient cellular uptake through receptor clustering.^{28,29} Upon endocytosis, the toxin part can be cleaved from the immunotoxin by the furin protease at the FCS in the early endosome and the enzymatic domain can reach the cytosol, where it finally inhibits translation.⁸ The cytotoxicity of the immunotoxins was highly specific to HER2 overexpressing cells with an efficacy of more than 65-fold compared to the toxin alone, or to HER2 low expressing or HER2 negative cells.

The present study describes a very straightforward process for generating an immunotoxin without chemical conjugation and additional purification steps to remove unreacted compounds and side products from the desired conjugation product. The association between E3 and K3 helices ensures a highly homogenous end product. In addition, this fully modular technology enables the replacement of the nano-HER2 moiety with any other target-specific binding domain to target other types of cancer cells. Finally, the possibility to produce both entities separately overcomes the solubility and yield issues of a full recombinant immunotoxin and offers the possibility

to express the target moiety in an eukaryotic organism, to achieve post-translational modifications if needed, for proper folding or activity.

Experimental procedures

Cell Lines

HCC1954, MDA-MB-231, BT474 and H9C2 (2-1) cell lines were maintained as monolayers in RPMI without Hepes, supplemented with 10 % fetal calf serum (FCS) and Gentamycin. MCF7, Caski, HeLa, MRC5 and SBKR cell lines were maintained as monolayers in Dulbecco's modified Eagle's medium (DMEM) (1 g/L Glucose) supplemented with 10 % fetal calf serum (FCS) and Gentamycin. For BT474 and MCF7, the medium was supplemented with 10 µg / ml Insulin.

Recombinant plasmid constructions

Nano-HER2 DNA sequences described elsewhere¹⁸ were amplified by PCR using HER2-For GATATACCATGGAAGTTCAACTGG and HER2-Rev ATGTGCACTAGTTGCGGCCGCAGAGCTAACCGTCACTTGGGTACC primers. HER2 PCR fragment was digested with NcoI-SpeI and ligated into the pETOM-P40M1-E3 or -K3 digested with NcoI-SpeI to replace the P40M1 sequences.¹⁶ An optimized sequence encoding for the TOX used in this study was synthesized by Integrated DNA Technologies (IDT) and amplified by PCR using specific primers: For-TOX TCTACTAGTGCAATGGGGTCTGGTGGCTGT and Rev-TOX: GAGCTTAAGAATAATGTTAAGTAGAAAG. The resulting PCR fragment digested with SpeI-EcoRI with has been then cloned into SpeI-EcoRI of the pETOM-E3 and pETOM-K3.¹⁶ The E3 and K3 sequences were amplified by PCR using NheI-K3-For GCTCGCTAGCGGTAACAACACCAGCTCCTCTC and HindIII-K3-Rev GCTCAAGCTTTTAACCCCCTGGCTCCTTCCCAGCC oligonucleotides and cloned into a pET6His-eGFP vector.

Expression and purification of the recombinant fusion proteins

Briefly, E3 and K3 fusion proteins were overexpressed in *E. coli* BL21 (DE3) pLysS with 0.5 mM isopropyl thiogalactoside (IPTG). After 24 h at 20°C, the cells were harvested, re-suspended 20 mM Phosphate buffer pH 8, 250 mM NaCl and 10 mM imidazole. Following lysis in a cell disruptor (Constant Systems Ltd), cell debris were removed by ultra-centrifugation, and the supernatant was applied to IMAC

chromatography charged with cobalt (GE Healthcare Saclay, France). IMAC purified proteins were subsequently loaded on HiLoad 16/60 Superdex 200 prep grade column or on Superdex 200 Increased 10/300 (GE Healthcare, Bio-sciences AB, Sweden) operating at a flow rate of 0.5 ml/ min. Fractions were separated on SDS-PAGE gels and analyzed by Coomassie blue. The heterotetramers were prepared by incubating together E3 and K3 targeted recombinant proteins at 1:1 molar ratio 5 min at RT followed in some experiments by a second purification on Superdex 200 Increased 10/300 GL size exclusion chromatography. Complex formation between labeled recombinant proteins was control by analytical chromatography on Superdex 200 Increased 5/150 GL.

Protein labeling

Recombinant proteins were labeled with either NHS-Ester Alexa488 dye using DyLight TM Microscale Antibody Labeling Kit following the protocol as described by the manufacturer (Thermo-Scientific, USA). Labeled proteins are indicated as [*] in text and figures.

***In vitro* protein transcription/translation inhibition assay.**

Inhibition of protein translation was performed using rabbit reticulocyte lysate (RRL) (Promega) and by measurement of luciferase activity. The assay was performed as suggested by the manufacturer (Promega) in a total volume of 15 μ l. Briefly, RRL was mixed with T7 expression plasmid encoding for the firefly luciferase and incubated for 90 min at 30 °C with or without increasing concentration of recombinant TOX. Then 5 μ l of each reaction were transferred to a black 96-well plate and assayed for luciferase activity, as previously described.³⁰ A control without any protein added served as positive control and was set as relative protein translation of 100 %. At least three independent experiments were carried out.

Circular Dichroism

CD experiments were performed at 20.0 ± 0.1 °C on a Jasco J-815 spectropolarimeter with 0.1 mm path-length quartz-Suprasil cells (JASCO Inc., Easton, MD USA). Acquisition parameters as continuous scan rate, response time, and bandwidth were 50 nm/min, 1.0 s, and 1 nm, respectively. The absorbance of the

buffer and the sample was kept as low as possible to ensure good signal-to-noise ratio. All spectra are systematically corrected by subtracting the solvent spectrum obtained under identical conditions.

Thermal Shift Assay

TSA experiments were carried out on real-time PCR systems (StepOnePlus; Applied Biosystems, Darmstadt, Germany). Purified nano-HER2, nano-HER2-E3 and nano-HER2-K3 were mixed with diluted Sypro Orange dye (final 2500-fold dilution from stock solution; Invitrogen, Carlsbad, CA, USA) in Phosphate Buffered Saline, pH 7.4 to a final volume of 20 μ l and a final protein concentration of 5 μ M. The samples were submitted to a denaturation kinetic from 25 to 95 °C at a rate of 1°C/min. The fluorescence of Sypro Orange dye was recorded in real time (excitation with a blue LED source and emission filtered through a ROX emission filter). The fluorescence profiles were fitted to a Boltzmann sigmoid equation to determine the melting temperature. Each experiment was repeated four times.

Dynamic Light Scattering analysis (DLS)

DLS was performed at 25°C using different protein concentration on a Malvern Zetasizer device (Malvernpanalytical). Results analysis was performed using Zetasizer software.

Transient siRNA transfections

Transient siRNA transfections were performed using Lipofectamine RNAiMAX (Invitrogen, P/N 56532) according to the manufacturer's instructions. STARD3-targeting siRNAs and HER2-targeting siRNAs were SMARTpool ON-TARGETplus obtained from Dharmacon. For controls, siRNAs ON-TARGETplus non-targeting pool from Dharmacon were used. siRNAs were used at 10 nM final concentration and cells were transfected 24 h - 72 h prior to experiments.

Fluorescence-Activated Cell Sorting (FACS)

Trypsinized cells were incubated with a mixture of equimolar ratio of recombinant proteins as indicated, for 30 min at 4 °C in PBS, 0.5% BSA, 2 mM EDTA. Cells were washed twice in PBS, 0.5% BSA, 2 mM EDTA and analyzed with

BD Accuri™ C6 Plus flow cytometer (BD Bioscience). The relative mean fluorescence intensities were normalized and plotted against the concentration of the nano-HER2 at monomer concentration. The data shown here are single point measurements.

Cytotoxicity Assay

5 000 cells were seeded per well in a 96-well plate and incubated for 24 h. Cells were then treated with increased concentrations of toxin, VHH, or immunotoxins. After 72 h, a crystal violet assay was conducted.³¹ The absorbance was measured in a Tecan reader (595 nm). IC₅₀ values were calculated by fitting a sigmoidal model with R software. Wells with cells treated with PBS were set at 100% of cell viability.

Supporting Information Available

DNA and proteins sequences, figures showing additional representations of the immunotoxin, purification steps and SEC analysis of recombinants proteins, thermal stability profiles, and cells viability assays with recombinant immunotoxin.

Acknowledgements

This work was supported by funds and/or fellowships from the Centre National de la Recherche Scientifique, the University of Strasbourg, the French Ministry of Research and the Ligue Régionale contre le Cancer (CCIR-GE). The CD device was funded with the help of the Association pour la Recherche sur le Cancer (ARC n.8008). Lucile GUYOT is supported by a grant from the French ANRT agency (CIFRE N°2018/1643). We thank C.L. Tomasetto and J.C. Amé for very helpful advises, and R. Wagner for the anti-HER2 nanobody clone.

References

(1) Romond, E. H., Perez, E. A., Bryant, J., Suman, V. J., Geyer, C. E., Davidson, N. E., Tan-Chiu, E., Martino, S., Paik, S., Kaufman, P. A., Swain, S. M., Pisansky, T. M., Fehrenbacher, L., Kutteh, L. A., Vogel, V. G., Visscher, D. W., Yothers, G., Jenkins, R. B., Brown, A. M., Dakhil, S. R., Mamounas, E. P., Lingle, W. L., Klein, P. M., Ingle, J. N., and Wolmark, N. (2005) Trastuzumab plus adjuvant chemotherapy for operable HER2-positive breast cancer. *N Engl J*

Med 353, 1673–1684.

- (2) Heyde, von der, S., Wagner, S., Czerny, A., Nietert, M., Ludewig, F., Salinas-Riester, G., Arlt, D., and Beissbarth, T. (2015) mRNA Profiling Reveals Determinants of Trastuzumab Efficiency in HER2-Positive Breast Cancer. *PLoS ONE* (Tan, M., Ed.) 10, e0117818.
- (3) Chakrabarty, A., Bhola, N. E., Sutton, C., Ghosh, R., Kuba, M. G., Dave, B., Chang, J. C., and Arteaga, C. L. (2013) Trastuzumab-Resistant Cells Rely on a HER2-PI3K-FoxO-Survivin Axis and Are Sensitive to PI3K Inhibitors. *Cancer Res* 73, 1190–1200.
- (4) Simon, N., and FitzGerald, D. (2016) Immunotoxin Therapies for the Treatment of Epidermal Growth Factor Receptor-Dependent Cancers. *Toxins* 8, 137.
- (5) Kreitman, R. J. (2006) Immunotoxins for targeted cancer therapy. *AAPS J* 8, E532–51.
- (6) Wayne, A. S., Fitzgerald, D. J., Kreitman, R. J., and Pastan, I. (2014) Immunotoxins for leukemia. *Blood* 123, 2470–2477.
- (7) Tsuchikama, K., and An, Z. (2016) Antibody-drug conjugates: recent advances in conjugation and linker chemistries 1–14.
- (8) Wolf, P., and Elsässer-Beile, U. (2009) Pseudomonas exotoxin A: From virulence factor to anti-cancer agent. *International Journal of Medical Microbiology* 299, 161–176.
- (9) Michalska, M., and Wolf, P. (2015) Pseudomonas Exotoxin A: optimized by evolution for effective killing. *Front. Microbiol.* 6, 958.
- (10) Amiri Tehranizadeh, Z., Sankian, M., Fazly Bazzaz, B. S., Chamani, J., Mehri, S., Baratian, A., and Saber, M. R. (2019) The immunotoxin activity of exotoxin A is sensitive to domain modifications. *Int. J. Biol. Macromol.* 134, 1120–1131.
- (11) Guo, R., Cao, L., Guo, W., Liu, H., Xu, H., Fang, Q., and Hong, Z. (2016) HER2-targeted immunotoxins with low nonspecific toxicity and immunogenicity. *Biochem Biophys Res Commun* 475, 93–99.
- (12) Pirzer, T., Becher, K.-S., Rieker, M., Meckel, T., Mootz, H. D., and Kolmar, H. (2018) Generation of Potent Anti-HER1/2 Immunotoxins by Protein Ligation Using Split Inteins. *ACS Chemical Biology* 13, 2058–2066.
- (13) Lee, S., Park, S., Nguyen, M. T., Lee, E., Kim, J., Baek, S., Kim, C. J., Jang, Y. J., and Choe, H. (2019) A chemical conjugate between HER2-targeting antibody fragment and Pseudomonas exotoxin A fragment demonstrates cytotoxic effects on HER2-expressing breast cancer cells. *BMB Reports* 52, 496–501.
- (14) Brox, R. D., Bolewska-Pedyczak, E., and Gariépy, J. (2003) A stable human p53 heterotetramer based on constructive charge interactions within the tetramerization domain. *J Biol Chem* 278, 2327–2332.
- (15) Brox, R. D., Bolewska-Pedyczak, E., and Gariépy, J. (2003) A Stable Human p53 Heterotetramer Based on Constructive Charge Interactions within the Tetramerization Domain. *J Biol Chem* 278, 2327–2332.
- (16) Vigneron, M., Dietsch, F., Bianchetti, L., Dejaegere, A., Nominé, Y., Cordonnier, A., Zuber, G., Chatton, B., and Donzeau, M. (2019) Self-Associating Peptides for Modular Bifunctional Conjugation of Tetramer Macromolecules in Living Cells. *Bioconjugate Chem.* 30, 1734–1744.
- (17) Kijanka, M., Warnders, F.-J., Khattabi, El, M., Lub-de Hooge, M., van Dam, G. M., Ntziachristos, V., de Vries, L., Oliveira, S., and van Bergen en Henegouwen, P. M. P. (2013) Rapid optical imaging of human breast tumour xenografts using anti-HER2 VHHs site-directly conjugated to IRDye 800CW for image-guided surgery. *Eur J Nucl Med Mol Imaging* 40, 1718–1729.
- (18) Hartmann, L., Botzanowski, T., Galibert, M., Jullian, M., Chabrol, E., Zeder Lutz, G.,

- Kugler, V., Stojko, J., Strub, J.-M., Ferry, G., Frankiewicz, L., Puget, K., Wagner, R., Cianferani, S., and Boutin, J. A. (2019) VHH characterization. Comparison of recombinant with chemically synthesized anti-HER2 VHH. *Protein Science* 5, 1122.
- (19) Hollevoet, K., Mason-Osann, E., Liu, X. F., Imhof-Jung, S., Niederfellner, G., and Pastan, I. (2014) In Vitro and In Vivo Activity of the Low-Immunogenic Antimesothelin Immunotoxin RG7787 in Pancreatic Cancer. *Molecular Cancer Therapeutics* 13, 2040–2049.
- (20) Bauss, F., Lechmann, M., Krippendorff, B.-F., Staack, R., Herting, F., Festag, M., Imhof-Jung, S., Hesse, F., Pompiati, M., Kollmorgen, G., da Silva Mateus Seidl, R., Bossenmaier, B., Lau, W., Schantz, C., Stracke, J. O., Brinkmann, U., Onda, M., Pastan, I., Bosslet, K., and Niederfellner, G. (2016) Characterization of a re-engineered, mesothelin-targeted Pseudomonas exotoxin fusion protein for lung cancer therapy. *Molecular Oncology* 10, 1317–1329.
- (21) Kaplan, G., Lee, F., Onda, M., Kolyvas, E., Bhardwaj, G., Baker, D., and Pastan, I. (2016) Protection of the Furin Cleavage Site in Low-Toxicity Immunotoxins Based on Pseudomonas Exotoxin A. *Toxins* 8, 217.
- (22) Sreerama, N., and Woody, R. W. (2000) Estimation of Protein Secondary Structure from Circular Dichroism Spectra: Comparison of CONTIN, SELCON, and CDSSTR Methods with an Expanded Reference Set. *Anal Biochem* 287, 252–260.
- (23) Wike-Hooley, J. L., Haveman, J., and Reinhold, H. S. (1984) The relevance of tumour pH to the treatment of malignant disease. *Radiother Oncol* 2, 343–366.
- (24) Pastrana, D. V., and Fitzgerald, D. J. (2006) A nonradioactive, cell-free method for measuring protein synthesis inhibition by Pseudomonas exotoxin. *Anal Biochem* 353, 266–271.
- (25) Freund, G., Sibler, A.-P., Desplancq, D., Oulad-Abdelghani, M., Vigneron, M., Gannon, J., Van Regenmortel, M. H., and Weiss, E. (2013) Targeting endogenous nuclear antigens by electrotransfer of monoclonal antibodies in living cells. *mabs* 5, 518–522.
- (26) Dai, X., Cheng, H., Bai, Z., and Li, J. Breast Cancer Cell Line Classification and Its Relevance with Breast Tumor Subtyping. *J. Cancer* 8, 3131–3141.
- (27) Behdani, M., Zeinali, S., Karimipour, M., Khanahmad, H., Schoonooghe, S., Aslemarz, A., Seyed, N., Moazami-Godarzi, R., Baniahmad, F., Habibi-Anbouhi, M., Hassanzadeh-Ghassabeh, G., and Muyldermans, S. (2013) Development of VEGFR2-specific Nanobody Pseudomonas exotoxin A conjugated to provide efficient inhibition of tumor cell growth. *New Biotechnology* 30, 205–209.
- (28) Moody, P. R., Sayers, E. J., Magnusson, J. P., Alexander, C., Borri, P., Watson, P., and Jones, A. T. (2016) Trigger Internalization and Lysosomal Targeting of Therapeutic Receptor:Ligand Complexes. *Molecular Therapy* 23, 1888–1898.
- (29) Wang, Q., Villeneuve, G., and Wang, Z. (2005) Control of epidermal growth factor receptor endocytosis by receptor dimerization, rather than receptor kinase activation. *EMBO Rep* 6, 942–948.
- (30) Diring, J., Camuzeaux, B., Donzeau, M., Vigneron, M., Rosa-Calatrava, M., Keding, C., and Chatton, B. (2011) A cytoplasmic negative regulator isoform of ATF7 impairs ATF7 and ATF2 phosphorylation and transcriptional activity. *PLoS ONE* 6, e23351.
- (31) Feoktistova, M., Geserick, P., and Leverkus, M. (2016) Crystal Violet Assay for Determining Viability of Cultured Cells. *Cold Spring Harb Protoc* 2016, pdb.prot087379.